



Green Chemical Oxidation Using Iron Nanoparticles for Removal of Azo Dye in Simulated Wastewater: Kinetics and Thermodynamics

Ahmed K. Hassan*, Mahdy S. Jaafar, Luay Q. Hashim, Ahmed M. Rezoqi, Mohammed F. Hashim

Environment and Water Directorate, Ministry of Science and Technology – Iraq

Article information

Article history:

Received: January, 03, 2023

Accepted: March, 12, 2023

Available online: October, 20, 2023

Keywords:

Green synthesis,
Iron nanoparticles,
Azo dye,
Fenton-like process,
Kinetics and thermodynamic

*Corresponding Author:

Ahmed K. Hassan

ahmedkhh71@gmail.com

DOI:

<https://doi.org/10.53523/ijoirVol10I2ID297>

This article is licensed under:

[Creative Commons Attribution 4.0 International License](https://creativecommons.org/licenses/by/4.0/).

Abstract

In this research, the greener catalyst of iron nanoparticles (G-FeNPs) was synthesized from the reduction of iron (III) salt by the extract of used green tea leaves waste. The product was characterized by SEM, AFM, and FTIR, while the zeta potential was measured to study the stability of G-FeNPs. The degradation of the anionic dye Eriochrome Blue Black R (EBBR) from an aqueous solution using a Fenton-like process catalyzed by G-FeNPs has been studied. The effects of catalyst dosage, hydrogen peroxide concentration, and pH, initial concentration of EBBR dye, contact time, and temperature were studied and evaluated for dye degradation. The optimized conditions achieved 91.5% removal of 25 mg/L EBBR dye at the reaction conditions: [G-FeNPs] = 0.8 g/L, [H₂O₂] = 4 mmol/L, pH=3, 60 min contact time, and at room temperature. Four kinetic models were employed to study the reaction kinetic model favorable; first-order, second-order, Elovich, and Behnajady-Modirshahla-Ghanbary (BMG). In general, Elovich and BMG reaction kinetics models are well fitted to all reactions. The thermodynamic functions, such as ΔG° , ΔH° , and ΔS° , were also investigated. The results obtained indicate that the Fenton-like process of EBBR dye was spontaneous and endothermic.

1. Introduction

Pollution of water resources with organic compounds is currently one of the finest environmental problems facing societies, mainly when it is to pollution or organic compounds existing in drinking water [1]. The discharging of organic pollutants which include fabric azo dye compounds in water systems is categorized as dangerous substances which could harm the nature of the ecosystem [2]. The maximum permissible limit of dye is less than 1.0 ppm in industrial discharge. It has been emphasized by many researchers that azo dyes have the ability to purpose allergenic, carcinogenic, mutagenic, and also reason numerous human sicknesses [3]. Therefore, it is very vital to lessen those organic compounds to the allowed limits earlier than they're discharged into water systems is crucial. Researchers maintain their efforts to develop green chemistry processes in easy, efficient, and reliable ways to produce nanomaterials. It's extraordinarily important to explore a more environmentally friendly and sustainable procedure for nanomaterials synthesis. Metal ions were reduced to metal nanoparticles using biologically active compounds consisting of polyphenols and flavonoids from plant extracts. In comparison to chemical and physical syntheses, this green bio-synthetic route is environmentally favourable due to, its low-cost, simple extraction, locally available, and socially acceptable. Many studies that

specialize in the use of biologically-active substances as a reducing agents which are extracted from natural plant leaves included: black and green tea leaves [4, 5], eucalyptus leaves [6], grape leaves [7], garlic vine leaves [8] and pomegranate (*Punica granatum*) leaves [9]. These bioactive substances extracted from leaves plants work as both reducing and capping agents to produce metal nanoparticles. The three main techniques for treating industrial wastewater that has been contaminated with different kinds of textile dyes are physical, chemical, and biological. Every technique has benefits and drawbacks, and occasionally there is only one available remediation option, and failure to accomplish the desired [10]. As a result, it is critical to discover a cost-effective and efficient technique to eliminate these contaminants and preserve the ecosystem and water sources. Classical Fenton oxidation, which is among the most widely used advanced oxidation processes has been widely used for removing the high load of different organic contaminates [11]. This process involves the generation of hydroxyl free radicals $\cdot\text{OH}$ as a result of the decomposition of hydrogen peroxide by ferrous ions (Fe^{2+}), the $\cdot\text{OH}$ considers a strong oxidizing agent and non-selectively degrades all of the organic pollutants and converts to CO_2 , H_2O , and inorganic salts [12]. The Fenton process has certain drawbacks, such as a narrow optimal pH range, a high amount of iron slurry generated, and issues with obtaining the homogeneous catalyst (Fe^{2+}) [12]. To overcome these obstacles associated with the classical homogenous Fenton process, the green heterogeneous Fenton process using a solid catalyst which is more frequently named a green Fenton-like process is proposed as an efficient, safe, eco-friendly, and cost-effective process [4].

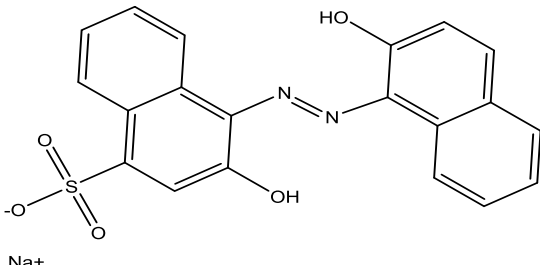
The aim of the present research focuses on developing and characterizing a greener catalyst of iron nanoparticles (G-FeNPs) synthesis from used green waste leaves and studying its performance in the current removal process for Eriochrome Blue Black R (EBBR) dye, which was subsequently studied in detail concerning the influence of some environmental parameters such as green catalyst dosage, hydrogen peroxide concentration, pH, contact time, temperature, and influence of various of EBBR dye concentrations on adsorption oxidation processes behavior, also studied four reaction kinetic models: first order, second order, Elovich [13], and Behnajady-Modirshahla-Ghanbary (BMG) [14], and thermodynamics reaction parameters..

2. Experimental Procedure

2.1. Materials and Solutions

All chemicals used in this study were of analytical reagent grade, and distilled water was used for preparing all solutions. The Eriochrome Blue Black R (EBBR) dye was provided by the Al-Kut Textile Factory, in Iraq. The main characteristics and chemical structure of EBBR dye are presented in Table (1). The wet green tea leaves waste was collected from home and dried at 50°C in an electric oven. Anhydrous ferric chloride (FeCl_3), hydrogen peroxide 30% weight per weight (H_2O_2), and sodium sulfite (Na_2SO_3) were obtained from Sigma-Aldrich. Sodium hydroxide (NaOH) and sulfuric acid (H_2SO_4) were used to adjust pH and were purchased from AppliChem (GmbH).

Table (1). The main characteristics and chemical structure of EBBR dye [15].

Dye	Eriochrome Blue Black R (EBBR)
Chemical structure	
Molecular formula	$\text{C}_{20}\text{H}_{13}\text{N}_2\text{NaO}_5\text{S}$
Molar Mass (g mol^{-1})	416.38
λ_{max} (nm)	530

2.2. Preparation of Green Iron Nanoparticles G-FeNPs

The G-FeNPs were prepared using a similar procedure described in the previous study [4] with some modifications. The procedure was as follows: The wet green tea leaves waste was collected and dried at 50°C in an electric oven. The bioactive extract was prepared by weighing 30.0 g of dry waste green tea leaves in 200 mL of distilled water. The solution was put in a microwave oven for 15 min. Then the extract was filtered using a 0.45- μm membrane filter to remove the suspended tea particles and stored in the refrigerator for further use. In the next step, a solution of 0.10 mol/L anhydrous ferric chloride was prepared by adding 3.25 g of solid FeCl_3 in 200 mL of distilled water. After complete dissolution, this solution was filtered with a 0.45 μm membrane filter to remove the impurities. The solution of green tea extract was added to the solution of 0.10 mol/L FeCl_3 through slow addition for 15 min at room temperature and was constantly stirred at a magnetic stirring rate of 300 rpm. After completing the addition, the color of the mixture changed from yellow to black, this indicated the reduction of Fe^{3+} to Fe^0 nanoparticles. Then the pH of the solution was adjusted to 6.0 and was constantly stirred for 15 min. After that, the solution was stood for one hour and the black precipitate of iron particles was collected through vacuum filtration with a filter paper with a 0.45- μm pore size and quickly rinsed several times with water and ethanol. The G-FeNPs were dried overnight in an oven at 50°C and then ground to a fine powder.

2.3. Characterization of G-FeNPs

The scanning electron microscope (SEM) model (TESCAN VEGA III), was used to characterize the morphology and distribution of the G-FeNPs. The atomic force microscope (AFM) was used to measure the surface morphology of nanoparticles [4, 16]. The Fourier transform infrared spectroscope (FTIR) spectra of the G-FeNPs in powdered form were recorded with a potassium bromide (KBr) pellet. A thin plate of G-FeNPs sample was prepared by mixing the sample with spectrally pure KBr. The FTIR analysis was performed with the Shimadzu spectrophotometer in the spectral range of 4000 to 400 cm^{-1} . The Zeta Potential Analyzer model (NanoBrook ZetaPlus) was used to evaluate the stability of synthesized iron nanoparticles by observing the electrophoretic behavior of the fluid. In any nanoparticles, the zeta potential can be ranged from positive at low pH values to negative at high pH values. The pH of the measured zeta potential was approximately 6.

2.4. Batch Experiments for Removal of EBBR Dye from Aqueous Solution

In this research, batch experiments were conducted to assess the removal efficiency of the degradation EBBR dye according to the following method [17]. In the Fenton-like experiments, the influence of hydrogen peroxide (H_2O_2) was studied in the range of 1.2 to 6 mmol/L on the degradation of 1000 mL of a synthetic solution with 75 mg/L EBBR dye at a pre-set G-FeNPs dosage of 0.8 g/L and pH of 3. Posteriorly, the effect of G-FeNPs dosages (in the range of 0.4-1.6 g/L) on the removal of EBBR dye solution (75 mg/L) was evaluated under the optimum H_2O_2 concentration (4 mmol/L) at a pH of 3. Experiments were carried out at four levels of pH (2, 3, 4, and 5) to search for the best pH for the decolorization of EBBR dye. Moreover, the effects of various concentration of EBBR dye on the heterogeneous Fenton-like oxidation were studied in the range of 25-100 mg/L under the optimum conditions ($[\text{H}_2\text{O}_2] = 4$ mmol/L, $[\text{G-FeNPs}] = 0.8$ g/L, and $\text{pH}=3$). Meanwhile, the reaction temperature was studied in the range of 20-40°C. The EBBR dye concentration during the Fenton-like reaction process was monitored by withdrawing 5-mL samples at fixed time intervals, filtering the samples with membrane filters of 0.22- μm pore size to remove the G-FeNPs catalyst, and transferring the samples to a glass vial containing 200 mL of 1 mol/L Na_2SO_3 to decompose excess H_2O_2 [14,18]. The absorbance of the EBBR dye solution was measured at λ_{max} 530 nm using UV-1700 spectrophotometer from Shimadzu, Japan. The calibration curve of the EBBR dye is provided in Figure (1). While removal efficiency percentage, R (%) for EBBR dye was calculated according to the below equation [19]:

$$R (\%) = \frac{C_0 - C_t}{C_0} \times 100 \quad (1)$$

where: C_0 (mg/L) is the initial concentration of EBBR dye, and C_t (mg/L) is the concentration of EBBR dye at time t (min).

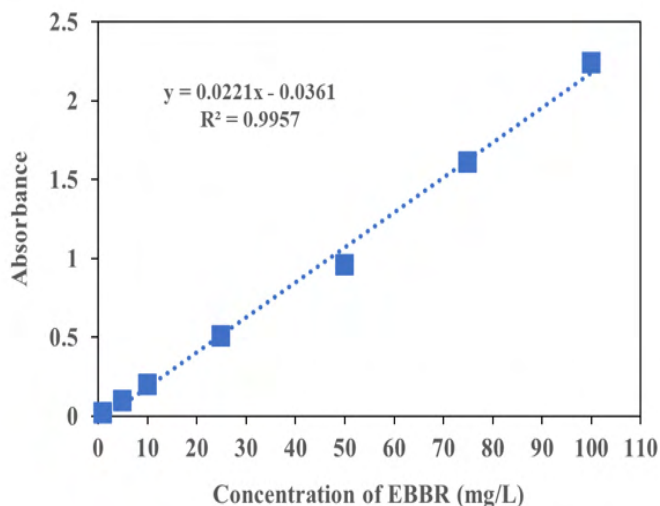


Figure (1). Calibration curve at various concentrations of EBBR dye solutions.

3. Results and Discussion

3.1. Characterization of G-FeNPs

The synthesized G-FeNPs were verified with the SEM and AFM analyses to investigate the diameter of the nanoparticles as shown in Figures (2) and (3). Figure (2) shows the SEM images of the green iron nanoparticles and this image depicted the morphology and distribution of G-FeNPs. Irregular spherical-shaped nanoparticles were found, probably owing to the existence of polyphenols on the surface of the nanoparticles. This agreement with the results of iron nanoparticles synthesis using the green tea leaves extract [20]. While, Figure (3), showed the AFM distribution and the particle size of synthesized iron nanoparticles G-FeNPs had an average diameter of less than 55 nm.

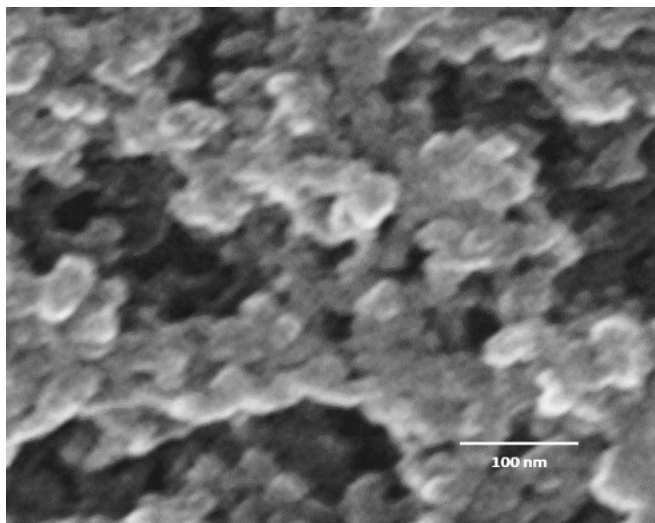


Figure (2). Scanning electron microscope (SEM) image of G-FeNPs.

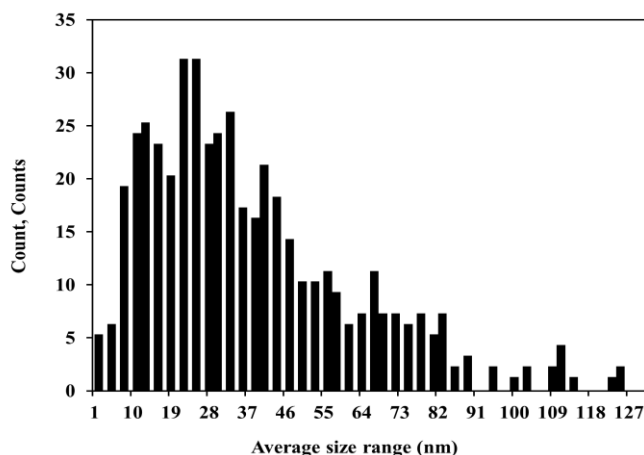


Figure (3). AFM distribution and the average particle size of G-FeNPs.

The stability of G-FeNPs in aqueous media was characterized by the zeta-potential analysis at pH=6. Zeta potential is a measurement technique of the effective electric charge on the nanoparticle's surface, quantifying the charges of these particles, and is based on the electrodynamics of solid-liquid dispersions [21]. Negative zeta potential of -28.36 mV was found for G-FeNPs as shown in Figure (4). This value indicates the low degree of coagulation of G-FeNPs, in terms of nanoparticles in environmental fluid stability, zeta potential value \pm (30-40) mV is considered stable and has moderate agglomeration [22].

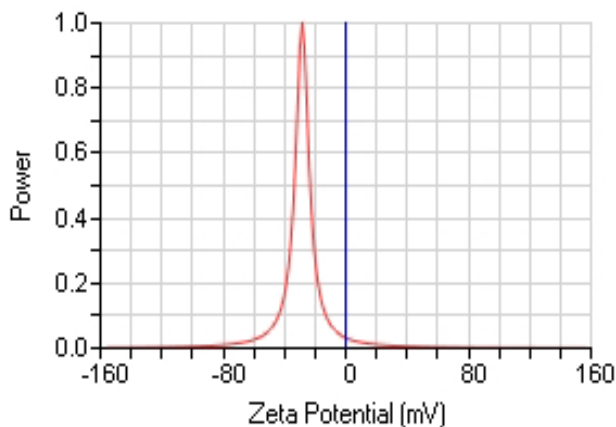


Figure (4). Zeta potential graphs for G-FeNPs.

The FTIR spectrum has recorded the wavenumber in the range of 4000 to 400 cm^{-1} for the green synthesized G-FeNPs as shown in Figure (5). The figure displays intense broadband stretching vibration at 3325 cm^{-1} for O-H and this indicates the presence of polyphenol compounds [4, 23]. The absorption intense band at 1618 cm^{-1} indicates the presence of a C=C aromatic ring stretching vibration, while the band of 1053 cm^{-1} denotes the existence of C-O-C symmetric stretching vibration of polyphenols [17]. The bands described above belonged to the characteristic peaks of green tea extracts. This indicates that the effective components in green tea extracts can be coated onto the surface of G-FeNPs.

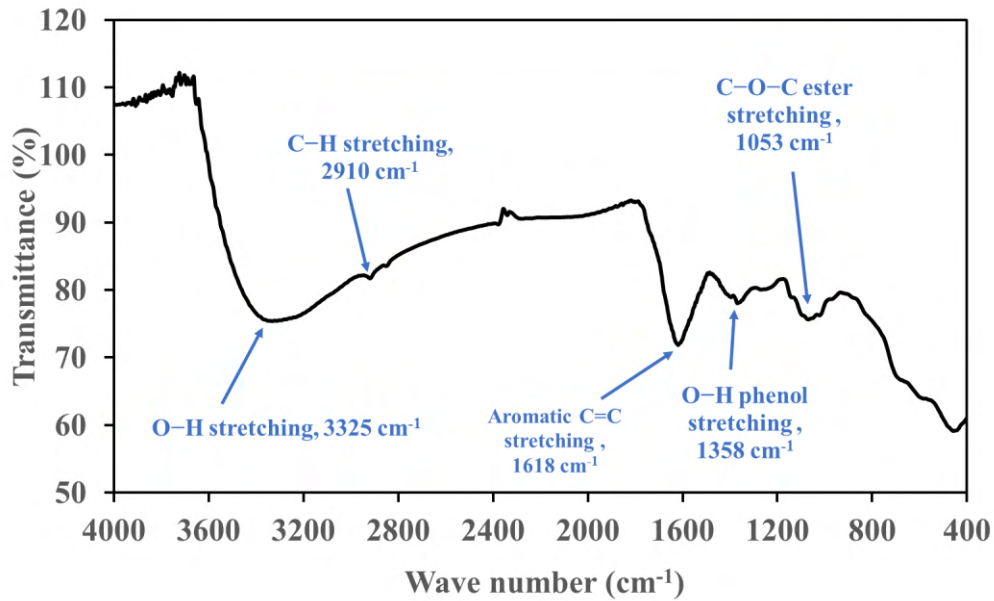


Figure (5). FTIR spectrum recorded for G-FeNPs.

3.2. The Effect of H₂O₂ Concentration Catalyzed By G-FeNPs on the Degradation of EBBR Dye

The concentration of hydrogen peroxide can directly affect the number of produced hydroxyl radicals and removal efficiency. Thus, it is very important to study the influence of H₂O₂ concentration on the removal efficiency of EBBR dye from aqueous solutions. The first step consists to fix the dose of G-FeNPs at 0.8 g/L and carrying out various experiments at different concentrations of H₂O₂ for the removal of 75 mg/L of EBBR dye at initial pH 3 and room temperature. Figure (6) represented the influence of four-level concentrations of H₂O₂ (1.2, 2, 4, and 6) mmol/L. The removal efficiency increased with an increase in the dose of H₂O₂, due to the high production of hydroxyl free radical ([•]OH) when increasing the hydrogen peroxide concentration. The values of removal percentage after 60 min of Fenton-like increased from 43.3% to 77.7% when increased hydrogen peroxide from 1.2 to 4 mmol/L, respectively (Figure (6) and Table (2)). There is no significant enhancement in the removal efficiency at a higher concentration of H₂O₂ 6 mmol/L, (see Table 2) this behavior may be attributed to the recombination of hydroxyl radicals with H₂O₂, and scavenging of [•]OH radicals will occur [14, 24]. Thus, the concentration of 4 mmol/L of H₂O₂ was chosen as the optimum concentration and was used in the next experiments.

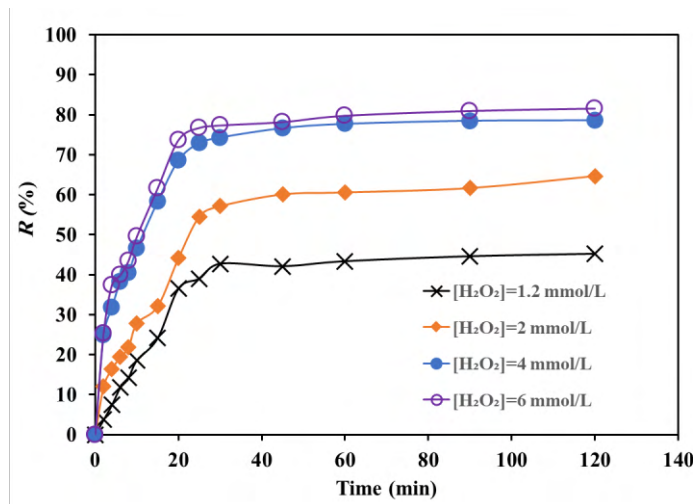


Figure (6). The removal efficiency of EBBR dye by various level concentrations of H₂O₂. Experimental condition: [EBBR] = 75 mg/L, [G-FeNPs] = 0.8 g/L, pH=3.0 and room temperature.

Four kinetic models were applied to calculate the degradation rate using the linear forms of the first-order, second-order, Elovich, and BMG kinetic models as shown in Eqs. (2) to (5), respectively [14].

$$\ln \frac{C_0}{C_t} = k_1 \cdot t \quad \text{First-order} \quad (2)$$

$$\frac{1}{C_t} - \frac{1}{C_0} = k_2 \cdot t \quad \text{Second-order} \quad (3)$$

where k_1 (min^{-1}) and k_2 ($\text{L}/(\text{mg} \cdot \text{min})$) are the kinetic rate constants of first and second-order kinetic models, respectively, C_0 and C_t are the concentration of EBBR dye (mg/L), at the initial and given time t (min).

$$C_t = C_0 + \frac{1}{\beta} \ln(\alpha \cdot \beta) + \frac{1}{\beta} \ln t \quad \text{Elovich} \quad (4)$$

where: β is extent of surface coverage (g/mg), α is rate of adsorption ($\text{mg}/(\text{g} \cdot \text{min})$) and t is time (min).

$$\frac{t}{[1 - (\frac{C_t}{C_0})]} = m + b \cdot t \quad \text{BMG} \quad (5)$$

where: m (min) and b are two constants concerning initial reaction rate and maximum oxidation capacity, respectively.

Also, Table (2), which represented the fitness of each kinetic model is determined by the determination regression coefficient (R^2). The best kinetic model is when the values of the correlation coefficient (R^2) draw closer to 1. Thus, the best kinetic model has the highest value of the determination R^2 .

Figure (7) showed the linear plots of kinetics data of the first-order, second-order, Elovich, and BMG models at different concentrations of H_2O_2 . All data are fitted well by the Elovich and BMG models because the correlation coefficient values of these models are mostly higher than those of the first-order and second-order kinetics models. These results are in agreement with previous research [25].

Table (2). First-order, second-order, Elovich, and BMG kinetic models regression coefficients, and removal efficiency at varying H_2O_2 , G-FeNPs, dosages, pH, and EBBR dye concentrations of Fenton-like oxidation.

[H_2O_2] (mmo/L)	[G-FeNPs] (g/L)	[EBBR] (mg/L)	pH	(R) , % After 60 (min)	Determination regression coefficient (R^2) of			
					First-order model	Second- order model	Elovich model	BMG model
1.2	0.8	75	3	43.3	0.794	0.815	0.923	0.817
2	0.8	75	3	60.5	0.859	0.890	0.932	0.908
4	0.8	75	3	77.7	0.807	0.886	0.966	0.984
6	0.8	75	3	79.7	0.770	0.842	0.957	0.986
4	0.4	75	3	35.1	0.967	0.984	0.928	0.845
4	1.2	75	3	75.0	0.836	0.931	0.988	0.988
4	1.6	75	3	71.2	0.928	0.975	0.970	0.950
4	0.8	75	2	78.6	0.592	0.769	0.768	0.999
4	0.8	75	4	57.5	0.829	0.888	0.965	0.942
4	0.8	75	5	39.0	0.963	0.980	0.914	0.742
4	0.8	100	3	57.7	0.912	0.951	0.971	0.874
4	0.8	50	3	83.2	0.773	0.886	0.953	0.994
4	0.8	25	3	92.7	0.715	0.908	0.800	0.999
Average R^2					0.826	0.900	0.922	0.925

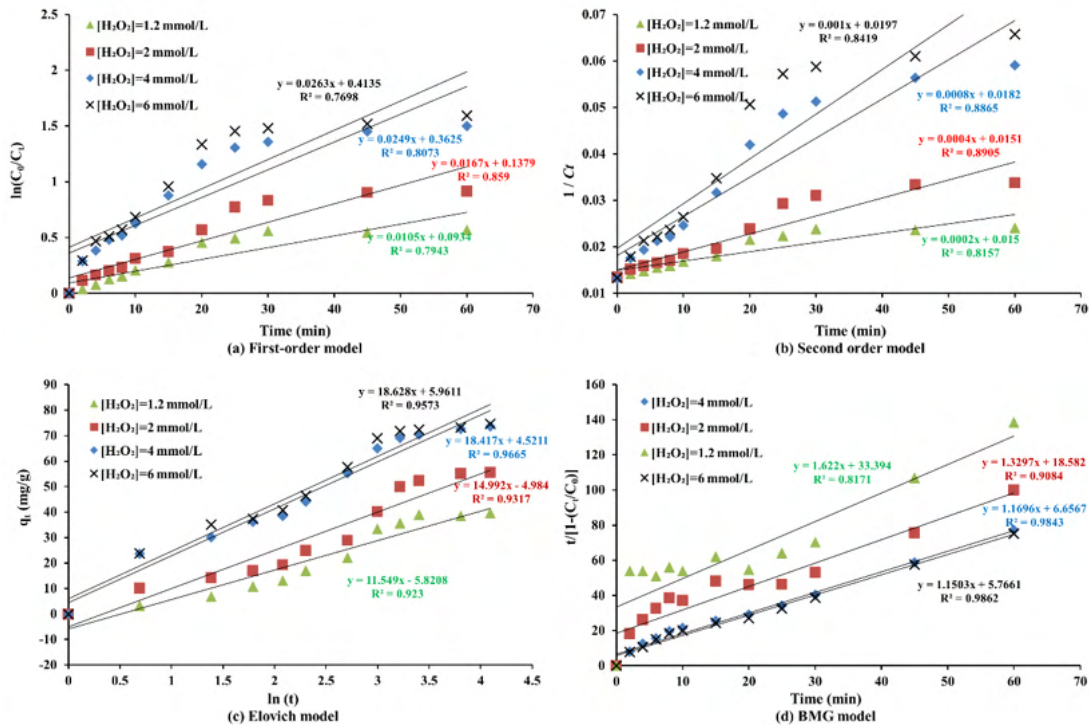


Figure (7). Linear plots of kinetics data of the first-order, second-order, Elovich, and BMG models at various concentrations of H_2O_2 .

3.3. The Effect of G-FeNPs on the Degradation of EBBR Dye

The dosages of G-FeNPs are a very important parameter to carry out the maximum removal efficiency of EBBR dye from aqueous solutions. The first step consists to remain the amount of H_2O_2 at the optimum concentration of 4 mmol/L and studying the influence of various amounts of G-FeNPs on the removal of 75 mg/L EBBR aqueous solution at initial pH 3.0 and room temperature. The effect of G-FeNPs concentration and oxidative reaction time on the degradation of the EBBR dye solution was illustrated in Figure (8). It is clear from Figure (8) and Table (2) that the removal efficiency for Fenton-like reaction for degradation of EBBR dye increased from 35.1% to 77.7% within 60 min reaction, when increasing the initial amount of G-FeNPs from 0.4 to 0.8 g/L, respectively. Further increase of the catalyst will decrease the removal efficiency, for example, increase the amount from 1.2 to 1.6 g/L led to a decrease in the $R\%$ of EBBR dye from 75% to 71.2%, respectively. Wang et al., 2016 [26] pointed out that the highest amount of catalyst in heterogeneous Fenton-like processes may have a negative effect during the treatment process, and this may be attributed to the scavenger of hydroxyl free radicals [4, 27].

The Elovich and BMG models provided the best fit based on the experimental data as summarized in Table (2) and Figure (9) for G-FeNPs catalyzed the Fenton-like oxidation process. In order to compare the different models, the “best-fit” model was determined by the high correlation coefficient, as shown in Figure (9) the kinetic models conform well to BMG model because the highest average R^2 value 0.986.

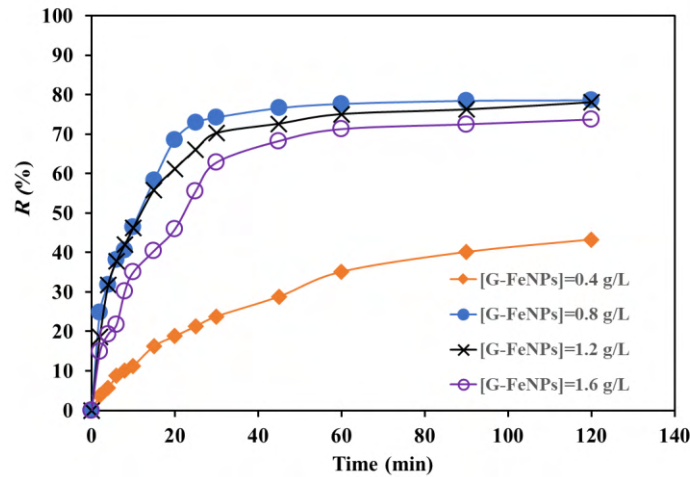


Figure (8). The removal efficiency of EBBR dye by various level concentrations of G-FeNPs. Experimental condition: [EBBR] = 75 mg/L, [H₂O₂] = 4 mmol/L, pH=3.0 and room temperature.

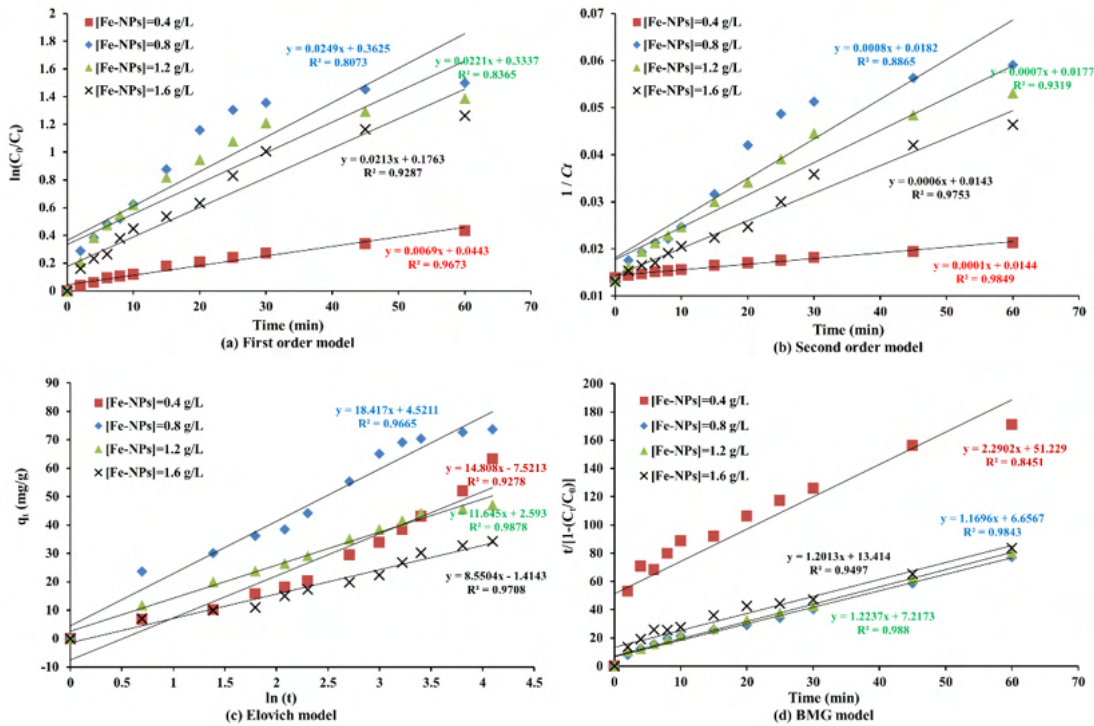
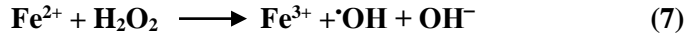
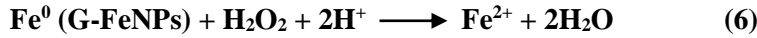


Figure (9). Linear plots of kinetics data of the first-order, second-order, Elovich, and BMG models at various dosages of G-FeNPs.

3.4. The Influence of pH on the Degradation of EBBR Dye

The pH influence is a highly important parameter for the operation Fenton-like oxidation treatment. However, from the previous studies, the acidic media of pH 2.5 to 3.5 consider achieving a better treatment efficiency [26]. Apparently, from Figure (10), and Table (2) the removal efficiency increased as the pH decreased from 5 to 2 indicating that pH has a strong influence on the degradation of EBBR dye, for example, the degradation increased from 39% to 78.6% for pH 5 and 2, respectively (Figure (10), Table (2)). This behavior may be explained in highly acidic media between 2 to 3 to the production of hydroxyl free radicals ($\cdot\text{OH}$), which are generated at a higher amount by the decomposition of hydrogen peroxide in an acidic state, as shown in Eqs. (6 and 7) [27].



Again, the kinetics parameters of the Elovich and BMG model have shown a high level of adjustment in all of the experimental tests, based on the values of coefficients (R^2) (Figure (11), Table (2)).

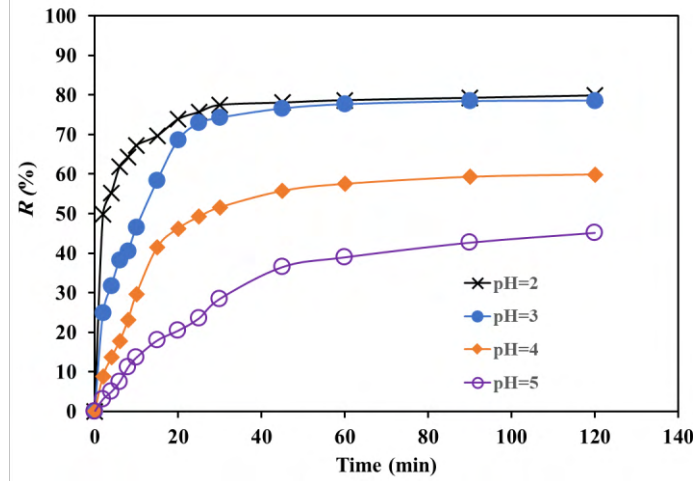


Figure (10). The removal efficiency of EBBR dye by various pH levels. Experimental condition: [EBBR] = 75 mg/L, [H₂O₂] = 4 mmol/L, [G-FeNPs] = 0.8 g/L and room temperature.

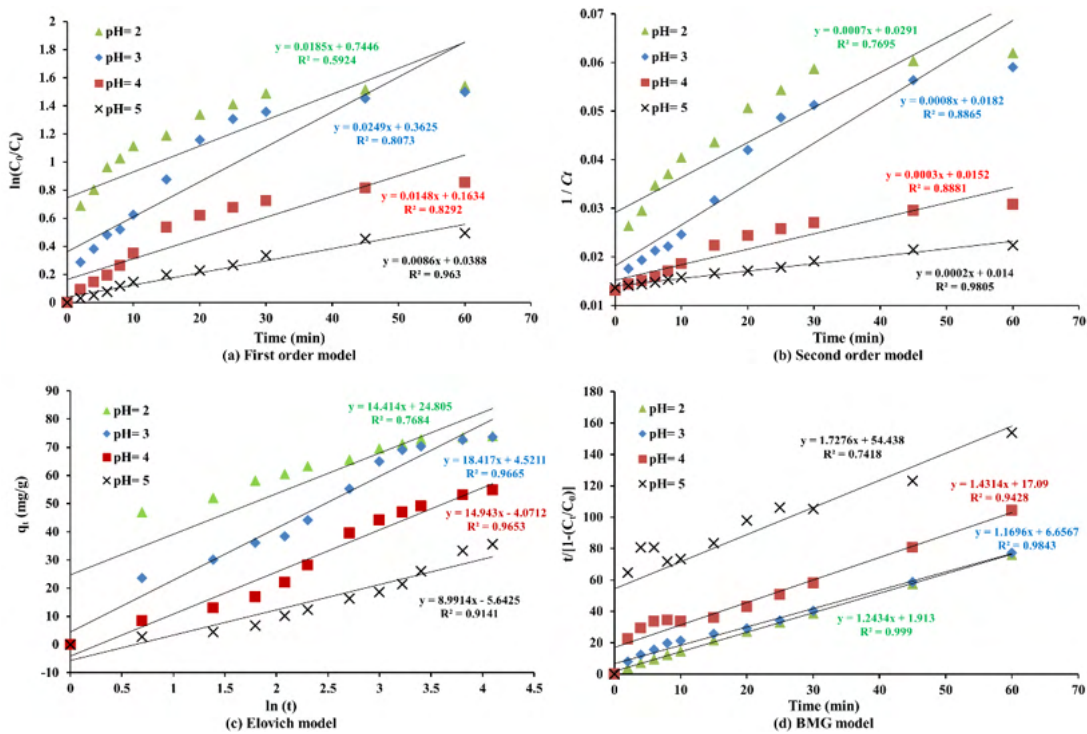


Figure (11). Linear plots of kinetics data of the first-order, second-order, Elovich, and BMG models at various pH levels.

3.5. The Influence of EBBR Dye Concentration

The effect of EBBR dye concentration has a significant effect on the treatment removal efficiency. Figure (12) represented the effect of varying EBBR dye concentrations on the Fenton-like treatment process. The result showed that the removal efficiency increased from (57.7% to 92.7%) when the initial EBBR dye concentration decreased from 100 to 25 mg/L, respectively (Table (2) and Figure (12)). It is concluded from Table (2) and

Figure (13) that the Elovich and BMG kinetic models have very good fitting these models due to the higher value of regression coefficients (R^2). Similar results were reported for the degradation of reactive red 120 dye using Fenton-like oxidation catalysed by green bimetallic nanoparticles (Fe/Ni) supported into zeolite 5A [23].

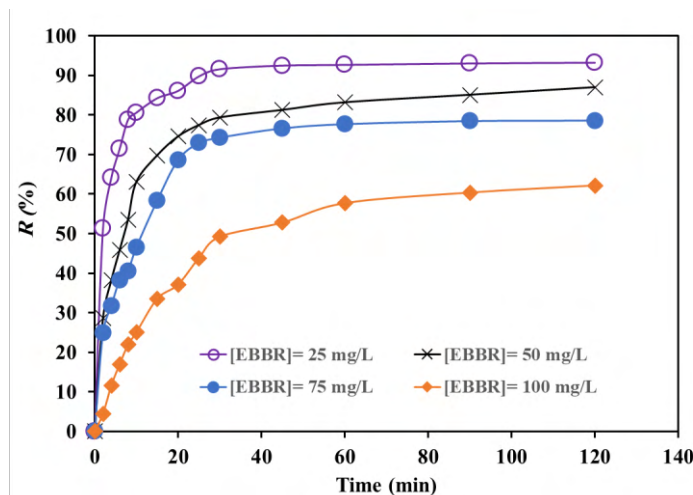


Figure (12). The removal efficiency of EBBR dye by various concentrations of EBBR dye. Experimental condition: $[H_2O_2] = 4 \text{ mmol/L}$, $[G\text{-FeNPs}] = 0.8 \text{ g/L}$, $\text{pH}=3$ and room temperature.

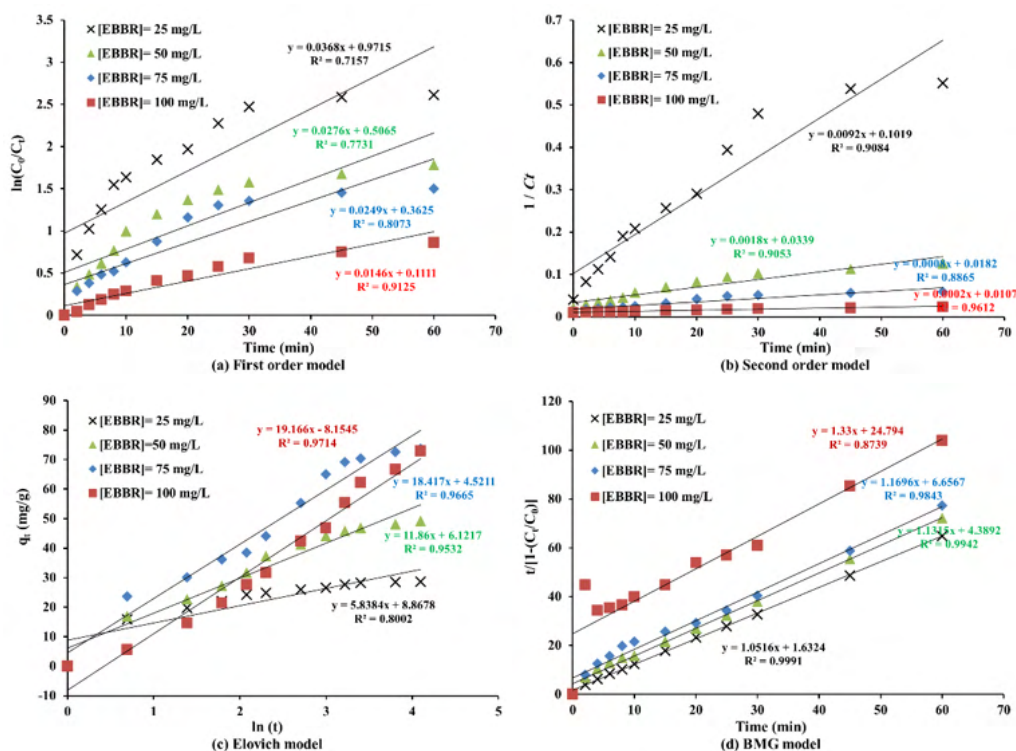


Figure (13). Linear plots of kinetics data of the first-order, second-order, Elovich, and BMG models at various concentrations of EBBR dye.

3.6. The Effect of Temperature on Degradation of EBBR Dye

In the Fenton-like oxidation process, the temperature of the reaction plays an important role in the treatment of organic pollutants [28]. From the experimental results presented in Figure (14) and Table (3), it can be seen that lowering the temperature has a negative effect on the removal efficiency of EBBR dye. For example, the removal efficiency within 60 min of a Fenton-like oxidation reaction decreased from 89.0% to 79.9%, as the temperature decreased from 40°C to 20°C (Table (3) and Figure (14)). This may be due to lower temperatures

will decrease the Fenton-like oxidation reaction rate between the G-FeNPs catalyst and H₂O₂, and that may be led up to a decrease in the formation of hydroxyl free radicals [29].

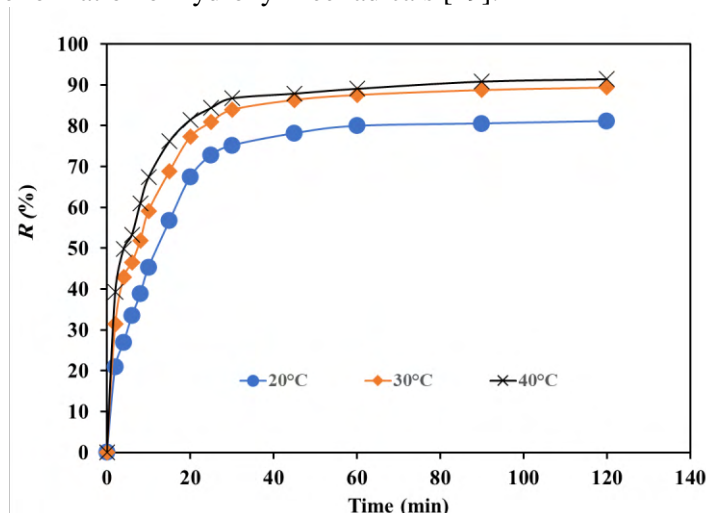


Figure (14). The removal efficiency of EBBR dye by various temperature. Experimental condition: [EBBR] = 75 mg/L, [H₂O₂] = 4 mmol/L, [G-FeNPs] = 0.8 g/L, and pH=3.

The values of the four kinetic models' parameters are summarized in Table (3). It can be seen from Figure (15), that the R^2 values obtained for the BMG and Elovich kinetic models were higher than first-order and second-order models, thus suggesting that quite adequately describe the data of experiments. It is concluded that the Elovich and BMG models have the best fitness considering that EBBR dye degradation by the Fenton-like oxidation process utilizing G-FeNPs catalyst obeys the Elovich and BMG kinetic models. In general, Elovich and BMG reaction kinetics models are well fitted to all reaction parameter systems, followed by a second-order reaction model due to the average $R^2 \geq 0.9$ (Table (2)).

Table (3). First-order, second-order, Elovich, and BMG kinetics models parameters for the removal of EBBR dye at various temperatures.

Temp. (°C)	(R), % after 60 (min)	First-order model		Second-order model		Elovich model			BMG model		
		k_1 (min ⁻¹)	R^2	k_2 (L/(mg.min))	R^2	α (mg/(g.min))	β (g/mg)	R^2	m (min)	b	R^2
20	79.9	0.0275	0.852	0.0010	0.933	20.186	0.0511	0.974	8.232	1.108	0.976
30	87.5	0.0340	0.843	0.0017	0.951	31.709	0.0510	0.962	4.703	1.064	0.991
40	89.0	0.0344	0.790	0.0019	0.924	44.455	0.0511	0.922	3.242	1.068	0.996
Average R^2			0.828		0.936			0.952			0.987

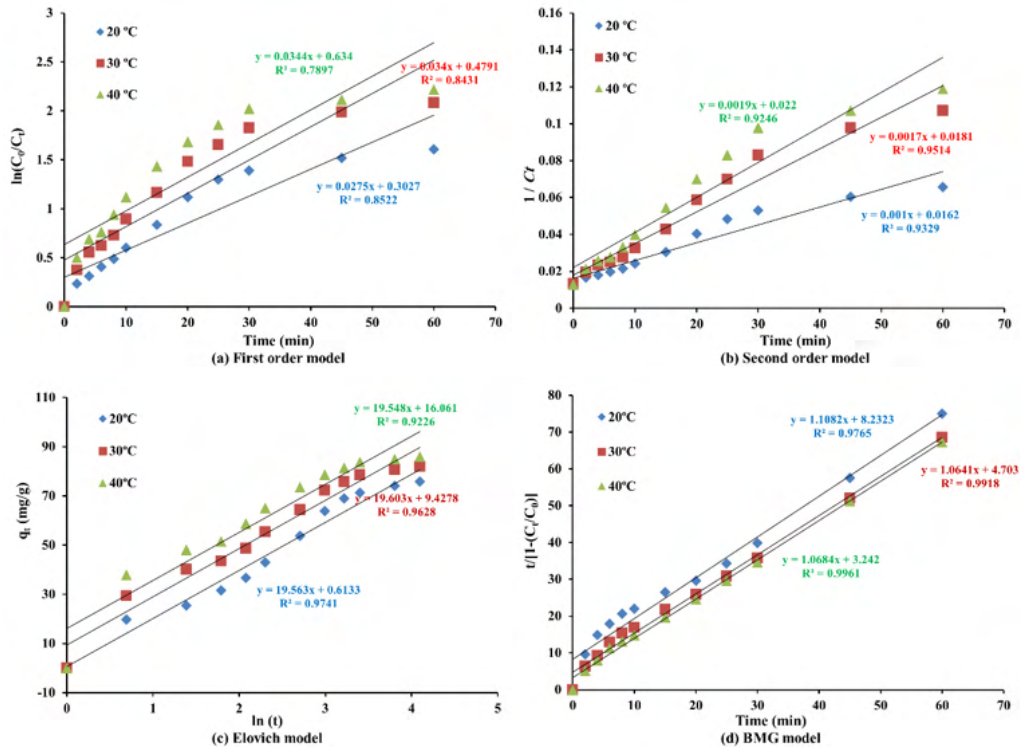


Figure (15). Linear plots of kinetics data of the first-order, second-order, Elovich, and BMG models at various temperatures.

3.7. Fenton-Like Thermodynamic Constants

The thermodynamic parameters standard Gibbs free energy change (ΔG^0), enthalpy change (ΔH^0), and entropy change (ΔS^0) for Fenton-like are calculated using the following equations [30]:

$$K_d = (C_0 - C_e) / C_e \times (V/m) \quad (8)$$

$$\Delta G^0 = -RT \ln K_d = \Delta H^0 - T\Delta S^0 \quad (9)$$

$$\ln K_d = (\Delta S^0 / R) - (\Delta H^0 / RT) \quad (10)$$

where T is the temperature of Fenton-like reaction in Kelvin, is the universal gas constant (8.314 J/mol.K), and K_d is the equilibrium constant (L/g) and can be obtained from Eq. 8, while C_e , V, and m are the concentration of EBBR dye at equilibrium, volume of solution in a liter, and amount of G-FeNPs in gram, respectively. The values of ΔG^0 can be calculated from Eq. 9, while ΔH^0 and ΔS^0 can be obtained from the plot of $\ln K_d$ versus $1/T$ as shown in Figure (16).

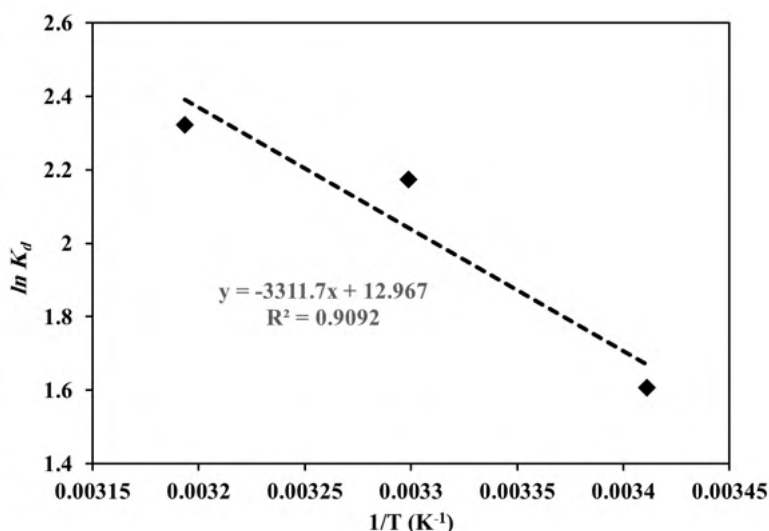


Figure (16). Relationship between $\ln K_d$ against $1/T$ for thermodynamic constants determination of removal EBBR dye by Fenton- like process. Experimental conditions: [EBBR] = 75 mg/L, [H₂O₂] = 4 mmol/L, [G-FeNPs] = 0.8 g/L, pH=3, and 60 min contact time.

Table (4) shows the negative values of ΔG^0 and positive ΔH^0 obtained indicated that the EBBR dye Fenton-like process is spontaneous and endothermic, respectively. From Table (4) the increasing temperature of the reaction led to an increase in the extent of the spontaneity of the Fenton-like oxidation process. The positive value of ΔS^0 indicates that the randomness increasing at the solid/solution interface occurs in the Fenton-like process of EBBR dye onto G-FeNPs catalyst. Similar result removal of malachite green dye by Fenton-like (Fe³⁺/H₂O₂) reaction at different temperatures 25–55°C. The results obtained that the Fenton-like process of malachite green dye was spontaneous and endothermic [19, 30].

Table (4). Thermodynamic functions ΔG^0 , ΔH^0 , and ΔS^0 .

Temperature (K)	K_d (L/g)	ΔG^0 (kJ/mol)	ΔH^0 (kJ/mol)	ΔS^0 (J/mol K)
293.15	4.983	-3.914	27.533	107.8
303.15	8.794	-5.479		
313.15	10.209	-6.048		

4. Conclusions

In this research, green waste leaves extract was used for the synthesis of iron nanoparticles. The structure of the formed G-FeNPs is confirmed by characterizations including SEM, AFM, and FTIR, while the stability of the product is confirmed by zeta potential. The removal efficiency was studied with the influence of process parameters including the pH and temperature of the media and the concentrations of G-NPs, H₂O₂, and the EBBR dye. The removal efficiency was 91.5% at experimental optimism conditions included: 0.8 g/L of G-FeNPs, 4 mmol/L of H₂O₂, and a 293.15 K temperature, besides a pH of 3.0 and an initial EBBR dye concentration of 25 mg/L after 60 min of Fenton-like oxidative reaction. The kinetic studies suggested that the Elovich and BMG models fitted better to all Fenton-like reaction parameters systems. The thermodynamic parameters of the Fenton-like system were investigated and the results showed that the Fenton-like reaction is highly spontaneous and endothermic.

Conflict of Interest: The authors declare that there are no conflicts of interest associated with this research project. We have no financial or personal relationships that could potentially bias our work or influence the interpretation of the results.

References

- [1] R. Tröger, P. Klöckner, L. Ahrens, and K. Wiberg, "Micropollutants in drinking water from source to tap- Method development and application of a multiresidue screening method," *Science of the Total Environment*, vol. 627, pp.1404-1432, 2018.
- [2] D.A. Yaseen and M.Scholz, "Textile dye wastewater characteristics and constituents of synthetic effluents: a critical review," *International journal of environmental science and technology*, vol. 16, no.2, pp.1193-1226, 2019.
- [3] K.T. Chung, "Azo dyes and human health: a review," *Journal of Environmental Science and Health, Part C*, vol. 34, no. 4, pp.233-261, 2016.
- [4] A. K. Hassan, G. Y. Al-Kindi, and D. Ghanim, "Green synthesis of bentonite-supported iron nanoparticles as a heterogeneous Fenton-like catalyst: Kinetics of decolorization of reactive blue 238 dye" *Water Science and Engineering*, vol. 13, no. 4, pp.286-298, 2020.
- [5] D. Ghanim, G. Y. Al-Kindi. and A. K. Hassan, "Green Synthesis of Iron Nanoparticles Using Black Tea Leaves Extract as Adsorbent for Removing Eriochrome Blue-Black B Dye" *Engineering and Technology Journal*, vol. 38, no. 10A, pp.1558-1569, 2020.
- [6] P. Salgado, D. O. Mártire, and G. Vidal, "Eucalyptus extracts-mediated synthesis of metallic and metal oxide nanoparticles: current status and perspectives," *Materials Research Express*, vol. 6, no. 8, p.082006, 2019.
- [7] F. Luo, Z. Chen, M. Megharaj, and R. Naidu, "Biomolecules in grape leaf extract involved in one-step synthesis of iron-based nanoparticles," *RSC Advances*, vol. 4, no. 96, pp.53467-53474, 2014.
- [8] A. S. Prasad, "Iron oxide nanoparticles synthesized by controlled bio-precipitation using leaf extract of Garlic Vine (*Mansoa alliacea*)," *Materials Science in Semiconductor Processing*, vol. 53, pp.79-83, 2016.
- [9] A. Rao, A. Bankar, A. R. Kumar, S. Gosavi, and S. Zinjarde, "Removal of hexavalent chromium ions by *Yarrowia lipolytica* cells modified with phyto-inspired Fe₀/Fe₃O₄ nanoparticles," *Journal of contaminant hydrology*, vol. 146, pp.63-73, 2013.
- [10] A.R.A. Giwa, I.A. Bello, A.B. Olabintan, O.S. Bello, and T.A. Saleh, 2020. "Kinetic and thermodynamic studies of fenton oxidative decolorization of methylene blue", *Heliyon*, vol. 6, no. 8, p.e04454, 2020.
- [11] A.D. Bokare, and W. Choi, "Review of iron-free Fenton-like systems for activating H₂O₂ in advanced oxidation processes". *Journal of hazardous materials*, vol. 275, pp.121-135, 2014.
- [12] S. Chakma, L. Das, and V.S. Moholkar, "Dye decolorization with hybrid advanced oxidation processes comprising sonolysis/Fenton-like/photo-ferrioxalate systems: a mechanistic investigation". *Separation and Purification Technology*, vol. 156, pp.596-607, 2015.
- [13] J. M. Jabar, Y. A. Odusote, K. A. Alabi, and I. B. Ahmed, "Kinetics and mechanisms of congo-red dye removal from aqueous solution using activated Moringa oleifera seed coat as adsorbent," *Applied Water Science*, vol.10, no. 6, pp.1-11, 2020.
- [14] A. K. Hassan, M. M. Rahman, G. Chattopadhyay, and R. Naidu, "Kinetic of the degradation of sulfanilic acid azochromotrop (SPADNS) by Fenton process coupled with ultrasonic irradiation or L-cysteine acceleration," *Environmental Technology & Innovation*, vol. 15, p.100380, 2019.
- [15] N. Zaghbani, M. Dhahbi, and A. Hafiane, "Spectral study of Eriochrome Blue Black R in different cationic surfactant solutions". *Spectrochimica Acta Part A: Molecular and Biomolecular Spectroscopy*, vol. 79, no. 5, pp.1528-1531, 2011.
- [16] M. A. Atiya, A. K. Hassan, and I. M. Luaibi, "Green Synthesis Of Bimetallic Iron/Copper Nanoparticles Using Ficus Leaves Extract For Removing Orange G (OG) Dye From Aqueous Medium." *Nature Environment & Pollution Technology*, vol. 21, no. 1, 2022.
- [17] A. K. Hassan, M. A. Atiya, and I. M. Luaibi, "A Green Synthesis of Iron/Copper Nanoparticles as a Catalytic of Fenton-like Reactions for Removal of Orange G Dye." *Baghdad Science Journal*, pp.1249-1249, 2022.
- [18] A. K. Hassan, A. F. Hassan, A. Jasim, and S. N. Owaiyd. "Treatment of Contaminated Textile Factories' Wastewater by Photocatalyst Degradation." *Iraqi Journal of Industrial Research*, vol. 9, no. 2, pp. 132-140, 2022.
- [19] A. K. Hassan, M. A. Atiya, and Z. A. Mahmoud. "Photo-Fenton-like degradation of direct blue 15 using fixed bed reactor containing bimetallic nanoparticles: Effects and Box–Behnken optimization." *Environmental Technology & Innovation*, vol. 28, pp. 102907, 2022.

- [20] L. Huang, X. Weng, Z. Chen, M. Megharaj, and R. Naidu. "Green synthesis of iron nanoparticles by various tea extracts: comparative study of the reactivity.", *Spectrochimica Acta Part A: Molecular and Biomolecular Spectroscopy*, vol. 130, pp.295-301, 2014.
- [21] S. E. Bourdo, R. Al Faouri, R. Sleezer, Z. A. Nima, A. Lafont, B. P. Chhetri, M. Benamara, B. Martin, G. J. Salamo, and A. S. Biris. "Physicochemical characteristics of pristine and functionalized graphene", *Journal of Applied Toxicology*, vol. 37, no. 11, pp.1288-1296, 2017.
- [22] J. Singh, T. Dutta, K. H. Kim, M. Rawat, P. Samddar, and P. Kumar. "'Green'synthesis of metals and their oxide nanoparticles: applications for environmental remediation," *Journal of nanobiotechnology*, vol. 16, no. 1, pp.1-24, 2018.
- [23] M. M. Abdul Hassan, S. Hassan, and K. A. Hassan "Green and chemical synthesis of bimetallic nanoparticles (Fe/Ni) supported by zeolite 5A as a heterogeneous Fenton-like catalyst and study of kinetic and thermodynamic reaction for decolorization of reactive red 120 dye from aqueous pollution", *Eurasian Chem Commun*, vol. 4, pp. 1062-1086, 2022.
- [24] C. S. Santana, M. D. Nicodemos Ramos, C. C. V. Velloso, and A. Aguiar, "Kinetic evaluation of dye decolorization by Fenton processes in the presence of 3-hydroxyanthranilic acid", *International Journal of Environmental Research and Public Health*, vol. 16, no. 9, 2019.
- [25] I. Fatimah, I. Sumarlan, and T. Alawiyah. "Fe (III)/TiO₂-montmorillonite photocatalyst in photo-Fenton-like degradation of methylene blue", *International Journal of Chemical Engineering*, vol. 2015, 2015.
- [26] N. Wang, T. Zheng, G. Zhang, and P. Wang, "A review on Fenton-like processes for organic wastewater treatment", *Journal of Environmental Chemical Engineering*, vol. 4, no. 1, pp.762-787, 2016.
- [27] B. Guo, T. Xu, L. Zhang, and S. Li, "A heterogeneous fenton-like system with green iron nanoparticles for the removal of bisphenol A: Performance, kinetics and transformation mechanism," *Journal of Environmental Management*, vol. 272, pp. 111047, 2020.
- [28] H.Y. Xu, Y. Wang, T. N. Shi, H. Zhao, Q. Tan, B. C. Zhao, X. L. He, and S.Y. Qi. "Heterogeneous Fenton-like discoloration of methyl orange using Fe₃O₄/MWCNTs as catalyst: combination mechanism and affecting parameters", *Frontiers of Materials Science*, vol. 12, no. 1, pp. 21-33, 2018.
- [29] R. Nicodemos, M. Daniel, L. A. Sousa, and A. Aguiar, "Effect of cysteine using Fenton processes on decolorizing different dyes: a kinetic study", *Environmental Technology*, vol. 43, no. 1, pp. 70-82, 2022.
- [30] S. Hashemian, "Fenton-like oxidation of Malachite green solutions: kinetic and thermodynamic study", *Journal of Chemistry*, vol. 2013, 2013.